A Generalized Battery Model of a Collection of Thermostatically Controlled Loads for Providing Ancillary Service

He Hao, Borhan M. Sanandaji, Kameshwar Poolla, and Tyrone L. Vincent

Abstract— The thermal storage potential of Thermostatically Controlled Loads (TCLs) is a tremendous flexible resource for providing various ancillary services to the grid. In this work, we study aggregate modeling, characterization, and control of TCLs for frequency regulation service provision. We propose a generalized battery model for aggregating flexibility of a collection of TCLs. A theoretical characterization of the aggregate power limits and energy capacity of TCLs is provided. Moreover, we propose a priority-stack-based control strategy to manipulate the power consumption of TCLs for frequency regulation, while preventing short cycling on the units. Numerical experiments are provided to show the accuracy of the proposed model and the efficacy of the developed control method.

I. INTRODUCTION

A sustainable energy future requires vastly greater penetration of renewable resources than the current level. Economic, environmental and political requirements have motivated many states in the United States as well as countries around the world to setup aggressive renewable portfolios [1]. As an example, the state of California has established a target by introducing 33% of renewables by 2020 [2]. The proper functioning of an electric grid requires continuous power balance between supply and demand, in spite of the randomness of system loads and the uncertainty of non-dispatchable generation.

However, increasing introduction of renewable energy supplies into the power grid imposes a challenge to maintain the power balance due to the volatility, intermittency, and uncontrollability of renewable resources. To ensure the functionality and reliability of the grid, more ancillary service procurements are required [3]–[5]. Among different ancillary services, regulation reserve and load following are the key services that have been considered for normal operating conditions of the grid. While load following handles more predictable and slower changes in load, regulation mitigates faster and unpredicted fluctuations in system load and uncontrolled generation. It was shown that if California achieved its 33% renewable penetration target, the regulation reserve

and load following requirements would triple [6], [7]. If these additional ancillary service procurements are provided by fossil fuel generators, it will increase undesired carbon emission and will be economically untenable. To this end, it is essential to explore the potential of the cleaner demand-side flexibility for ancillary service.

Residential Thermostatically Controlled Loads (TCLs) such as air conditioner, heat pump, water heater, and refrigerator contribute to about 20% of the total electricity consumption in the United States [8], [9]. The large thermal storage capabilities of TCLs present an enormous potential for providing various ancillary services to the grid.

A. Related Work

The study of aggregate behavior of a large population of TCLs can date back to the 1980s. In [10], a physically based modeling was proposed to study the cold load pickup and payback phenomena of TCLs after a power outage. Malhame and Chong used a system of coupled Fokker-Planck equations to model the probability density of the temperature evolution of a large population of TCLs [11]. The aggregation of TCLs has also received a lot of attention more recently. Several papers have studied modeling and control of residential TCLs for load following, secondary regulation control, and energy arbitrage [12]–[18]. Provision of ancillary service by residential pool pumps was also considered in [19].

In fact, some utility companies have already harnessed the flexibility of TCLs for demand response. For example, the SmartAC™ program initiated by PG&E (Pacific Gas and Electric Company) gathered 147,600 residential customers for peak load shaving and managing emergency situations [20]. However, these load control mechanisms implemented in utilities are primarily concerned with low frequency changes in demand, i.e., the changes occur over hours timescale. There is an enormous additional potential for fast ancillary service (such as regulation) that is virtually not exploited.

In this paper, we study aggregating the flexibility in the deployment of residential TCLs to provide regulation service to the grid. Frequency regulation is one of the most important ancillary services to maintain the power balance. It is deployed on the fastest time scales (seconds to one minute) to compensate the power imbalance between system-side generation and load. Moreover, frequency regulation is a capacity service; the regulation signal is typically a zero-mean signal [21], with little energy requirement [22]. This makes flexible loads with circumscribed storage capabilities

such as TCLs the perfect demand-side resource for providing regulation service.

B. Main Contributions

One of the main contributions of this paper is that we propose a generalized battery model for aggregating flexibility of a collection of TCLs. Based on the proposed generalized battery model, we provide a theoretical characterization of the aggregate power limits and energy capacity for a collection of TCLs. We show that the aggregate flexibility of a population of heterogeneous TCLs can be bounded by two battery models, where the gap between the two battery models diminishes as the amount of heterogeneity goes to zero. This model provides a simple and convenient framework for system operators to allocate power and dispatch energy for ancillary service provision. To the best of our knowledge, our work is the first paper to analytically characterize the flexibility of TCLs. A simulation based estimation on the potential of TCLs was reported in [18].

Another contribution is that we propose a priority-stack-based control strategy to control a population of TCLs for frequency regulation. In each of the two priority stacks (one stack is considered for the ON units and one for the OFF units), the unit that is closer to its lower (upper) temperature bound is assigned with a higher priority to be switched OFF (ON) for service provision. A similar temperature-based preference control approach, and a time-based priority control method were also independently developed in [14], [17]. Moreover, the priority-stack-based control strategy prevents short cycling on each unit, and reduce the wear and tear on the equipment. The developed control method presents an excellent tracking performance and high robustness to uncertainties.

C. Paper Organization

The remainder of the paper is organized as follows. The mechanism by which TCLs are aggregated to provide regulation reserve is presented in Section II. Section III describes the thermal dynamics of an individual TCL. In Section IV, we propose a generalized battery model for a collection of TCLs, and characterize their aggregate flexibility. Priority-stack-based control of TCLs is presented in Section V. Section VI is devoted to numerical experiments. The paper ends with conclusions and future work in Section VII.

II. CONTROL ARCHITECTURE FOR AN AGGREGATION OF TCLS

In this paper, we study how to provide frequency regulation service to the grid via control of an aggregation of TCLs. The regulation signal or AGC (Automatic Generation Control) command, which is denoted by $r(t)$, is typically a sequence of pulses at 4-second intervals. The magnitude of the regulation signal indicates the amount of power asked by the system operator.

Thanks to the large thermal storage capabilities of TCLs, a significant amount of flexibility potential can be exploited for regulation service provision. The TCLs provide the function of keeping their internal temperature within specific bounds. Under the nominal, local control, there is a specific average
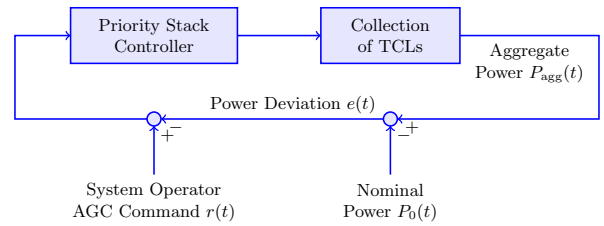

Fig. 1. Control architecture of TCLs for regulation service provision.

power that is required to achieve this function. For a large collection of TCLs that is uncoordinated, the instantaneous power drawn by this collection will be very close to the combined average power requirement, because any specific TCL will be at a random point along its operating cycle. However, if the TCLs can respond to the signals of a system operator, the aggregate instantaneous power can be made to be quite different from the average. For example, if the system operator requires more power in the grid, the aggregation of TCLs can "discharge" power by turning OFF some of the ON units. Similarly, an aggregation of TCLs can also absorb power from the grid by turning ON some of the OFF units. The difference between the instantaneous and average power is thus available to provide regulation reserve to the grid.

In this paper, we adopt a centralized control architecture, in which each TCL receives signals from a control authority who has the ability to override their local control actions. To provide frequency regulation service, at each sample time (every 4 seconds), the system operator compares the regulation signal $r(t)$ with the power deviation of a population of TCLs, $e(t) = P_{agg}(t) - P_0$, where $P_{agg}(t)$ is the instantaneous power drawn by the coordinated aggregation, and P_0 is the average power that would have been drawn by the uncoordinated aggregation. If $r(t) > e(t)$, the population of TCLs needs to "discharge" power to the grid, which means some of the units will be turned OFF. On the contrary, if $r(t) < e(t)$, then the population of TCLs needs to absorb more power from the grid by turning ON some of the OFF units. A priority-stack-based control strategy (that will be described in Section V) is used to determine the appropriate switching action of each TCL to prevent short-cycling and reduce wear and tear of the mechanical equipment. The overall control architecture is depicted in Fig. 1.

To implement such a control architecture, measurements of power and temperature of each TCL are required at a minimum sampling rate of 0.25 Hz to determine appropriate control actions. This feedback control strategy has a great advantage of dealing with modeling errors and external disturbances from occupancy, solar radiation, and so on. While the temperature is readily available from the thermostat, measuring the power consumption of each TCL necessitates nontrivial capital cost. Power meters are expensive. *In our view, this is unavoidable.* Other schemes have been proposed where the aggregate power is *estimated* using population models, or disaggregated from substation measurements. These are either open-loop control strategies, or result in unreliable tracking of the regulation signal. These schemes also face challenges in meeting the stringent auditing and

telemetry requirements necessary to participate in the ancillary service markets [23].

III. INDIVIDUAL TCL MODEL

In this section, we first present a hybrid model for TCLs, in which the power input of each unit has ON-OFF switching behavior. We next consider a continuous model with continuous power input to facilitate the ensuing analysis. We conjecture that in the limit of large population, the aggregate behavior of a collection of TCLs with the hybrid model can be approximated by that with the continuous model. Numerical experiments using the hybrid model will be given to support our analysis based on the continuous model.

A. Hybrid Model

Consider a population of N TCLs. The temperature evolution of each TCL (indexed by k) can be described as

$$C^k \frac{d\theta^k(t)}{dt} = \frac{\theta_a - \theta^k(t)}{R^k} - m^k(t)P^k\eta^k + w^k(t), \quad (1)$$

where $\theta^k(t)$ is the internal temperature of the k-th TCL, C^k and R^k are respectively its thermal capacitance and thermal resistance, θ_a is the ambient temperature, and m^k is a dimensionless binary variable that indicates the operating state of each TCL (1 when it is ON and 0 when it is OFF). In addition, P^k is the rated power, and η^k is its coefficient of performance. Without loss of generality, P^k is positive for cooling mode, and it is negative for heating mode. The first term on the right-hand side of (1), $(\theta_a - \theta^k(t))/R^k$, represents the heat conduction with the ambient, the second term $P^k\eta^k$ denotes the rate of energy transfer when it is ON, and the last term $w^k(t)$ accounts for external disturbances such as occupancy and solar radiation. Table I describes the parameters and their typical values for a residential air conditioner.

TABLE I
TYPICAL PARAMETER VALUES FOR A RESIDENTIAL AC UNIT [24].

Parameter	Description	Value Range	Unit
C	thermal capacitance	$1.5 - 2.5$	kWh/°C
R	thermal resistance	$1.5 - 2.5$	°C/kW
P	rated electrical power	$4 - 7.2$	kW
η	coefficient of performance	2.5	
θ_r	temperature setpoint	$18 - 27$	°C
δ	temperature deadband	$0.25 - 1.0$	°C

Each TCL has a temperature setpoint θ_r^k with a hysteretic ON/OFF local control within a deadband $[\theta_r^k - \delta^k/2, \theta_r^k + \delta^k/2]$. In the cooling mode, the operating state $m^k(t)$ evolves as

$$m^k(t + \Delta t) = \begin{cases} 0 & \text{if } \theta^k(t + \Delta t) < \theta_r^k - \delta^k/2, \\ 1 & \text{if } \theta^k(t + \Delta t) > \theta_r^k + \delta^k/2, \\ m^k(t) & \text{otherwise,} \end{cases}$$

where $\Delta t \ll 1$ is a small time increment. Additionally, the aggregated power consumption of a collection of TCLs at time t is given by

$$P_{\text{agg}}(t) = \sum_{k=1}^{N} m^k(t)P^k. \quad (2)$$

We define T_{ON}^k as the time it takes for the k-th TCL to transport from its upper temperature bound $\theta_r^k + \delta^k/2$ to its lower temperature bound $\theta_r^k - \delta^k/2$. From Model (1), it is straightforward to show that

$$T_{\text{ON}}^k := R^k C^k \ln \frac{\theta_r^k + \delta^k/2 - \theta_a + R^k P^k \eta^k}{\theta_r^k - \delta^k/2 - \theta_a + R^k P^k \eta^k}.$$

Similarly, T_{OFF}^k is defined as the time it takes for the k-th TCL to transport from its lower temperature bound to its upper temperature bound,

$$T_{\text{OFF}}^k := R^k C^k \ln \frac{\theta_r^k - \delta^k/2 - \theta_a}{\theta_r^k + \delta^k/2 - \theta_a}.$$

Consequently, the duty cycle of the k-th TCL is defined as

$$d^k := \frac{T_{\text{ON}}^k}{T_{\text{ON}}^k + T_{\text{OFF}}^k}.$$

The average power consumed by the k-th TCL over a cycle is defined as

$$P_a^k := P^k d^k = \frac{P^k T_{\text{ON}}^k}{T_{\text{ON}}^k + T_{\text{OFF}}^k}. \quad (3)$$

At steady-state, the number of TCLs that are ON is a constant. Their aggregate baseline power is given by

$$P_0 \equiv \sum_{k=1}^{N} P_a^k. \quad (4)$$

B. Continuous Model

As an approximation to the hybrid model, we consider a continuous thermal model, in which each TCL has continuous power input $m^k(t)P^k \in [0, P^k]$ instead of binary values of $\{0, P^k\}$. Equivalently, the continuous thermal model without disturbance $w^k(t)$ can be written as

$$\dot{\theta}^k(t) = a^k(\theta_a - \theta^k(t)) - m^k(t)b^k P^k, \quad (5)$$

where $a^k = \frac{1}{C^k R^k}, b^k = \frac{\eta^k}{C^k}$. Note that in this model, as common in the literature, the disturbance w is assumed to be zero mean [11], [12], [14], and thus neglected. If a non-zero mean existed, it could be approximated by an appropriate change to θ_a. Maintaining the temperature $\theta^k(t)$ within the user-specified dead-band $\theta_r^k \pm \delta^k/2$ is treated implicitly as a *constraint* on the power input. When evaluating the trajectory $\theta^k(t)$, it is assumed that $\theta^k(0) = \theta_r^k$. The nominal power to keep a TCL at its setpoint is given by

$$P_0^k := \frac{a^k(\theta_a - \theta_r^k)}{b^k} = \frac{\theta_a - \theta_r^k}{\eta^k R^k}. \quad (6)$$

Fig 2 compares the average power P_a^k given in (3) and the nominal power P_0^k given in (6) for different ambient temperatures. We observe that the two match each other very well. As a result, the average power consumed by the hybrid model, P_a^k, can be accurately approximated by the nominal power of the continuous model, P_0^k. Consequently, the baseline power of a population of TCLs with the hybrid model can be approximated by the aggregate nominal power of TCLs with continuous model, i.e., $P_0 \approx \sum_k P_0^k$.
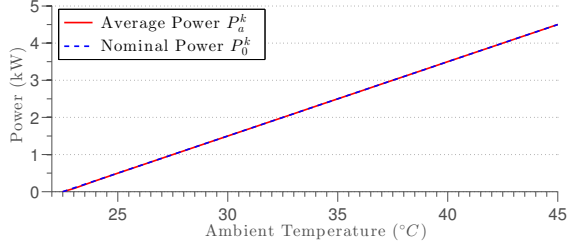
Fig. 2. Comparison of the average power P_a^k and the nominal power P_0^k for an air conditioner with different values of ambient temperature. The air conditioner parameters used are taken as the mean of the values in Table I.

IV. GENERALIZED BATTERY MODEL OF AGGREGATE FLEXIBILITY

To fully harness the flexibility benefits from TCLs, it is essential to characterize the potential of their aggregate power limits and energy capacity. In this section, we present compact, intuitive models for energy storage devices that will be very useful for expressing the capabilities of an aggregation of TCL units. The models given here will be expressed in the form of sets, that is, the model will be described in terms of the set of valid power signals that could be supported by the energy storage device. All proofs in this section are given in the Appendix.

A. Generalized Battery Model

Definition 1: A *Generalized Battery Model* $\mathbb{B}$ is a set of signals $u(t)$ that satisfy

$$-n_- \leq u(t) \leq n_+, \quad \forall\, t > 0,$$
$$\dot{x} = -ax - u,\ x(0) = 0 \ \Rightarrow |x(t)| \leq C, \quad \forall\, t > 0.$$

The model is specified by the non-negative parameters C, n_-, n_+, a. $\qquad\square$

Note that the parameters C, n_-, n_+, and a respectively denote the battery's energy capacity, its lower power limit, its upper power limit, and its dissipation rate. The variable $x(t)$ defines the State of Charge (SoC) of the battery.

A single TCL unit is easily shown to be a generalized battery when the input is taken to be the difference between the instantaneous power and nominal power, $e^k(t) = m^k(t)P^k - P_0^k$. Define $\phi^k := C^k(\theta^k - \theta_r^k)/\eta^k$. The continuous model (5) can be rewritten as

$$\dot{\phi}^k(t) = -a^k\phi^k(t) - e^k(t). \qquad (7)$$

Apparently, the TCL described by model (7), supports the set of power signals $e^k(t)$ in the set $\mathbb{E}^k = \mathbb{B}(\Delta^k, m_-^k, m_+^k, a^k)$, with

$$\Delta^k = \frac{C^k\delta^k}{2\eta^k}, \quad m_-^k = P^k - P_0^k, \quad m_+^k = P_0^k. \qquad (8)$$

An aggregator will have the opportunity to assign power signals to each of the TCLs in their collection with the aim that the sum achieves an overall power trajectory $u(t)$. The set of aggregate power signals that are achievable will satisfy the model $u(t) \in \mathbb{U}$ where

$$\mathbb{U} = \left\{ u(t) = \sum_k e^k(t) \Big| e^k(t) \in \mathbb{E}^k,\ \forall\, k \right\}.$$

We wish to characterize this aggregation as a generalized battery with power signal u. This is the subject of the next section.

B. Characterizing the Flexibility of a collection of TCLs

We consider a population of *heterogeneous* TCLs with unit generalized battery model $\mathbb{E}^k$ and aggregate model $\mathbb{U}$. We will find generalized battery models $\mathbb{B}_n$ and $\mathbb{B}_s$ that provide upper and lower bounds on $\mathbb{U}$, that is

$$\mathbb{B}_s \subseteq \mathbb{U} \subseteq \mathbb{B}_n.$$

The first result gives an upper bound.

Theorem 1: Consider a collection of *heterogeneous* TCLs, $\mathbb{E}^k = \mathbb{B}(\Delta^k, m_-^k, m_+^k, a^k)$ with aggregate model $\mathbb{U}$. Then $\mathbb{U} \subset \mathbb{B}_n = \mathbb{B}(C, n_-, n_+, a)$, where the parameters of $\mathbb{B}_n$ are given by

$$C = \sum_k (1 + |1 - \frac{a^k}{a}|)\Delta^k,$$
$$n_- = \sum_k m_-^k, \quad n_+ = \sum_k m_+^k,$$

and a is an arbitrary positive real number. $\qquad\square$

This upper bound provides a necessary condition for $u(t)$ to be achievable by the aggregator. If $u \notin \mathbb{B}_n$, then there is no possible assignment of e^k that could achieve $u = \sum_k e^k$.

We next give parameters of a generalized battery such that $\mathbb{B}_s \subset \mathbb{U}$.

Theorem 2: Consider a collection of *heterogeneous* TCLs, $\mathbb{E}^k = \mathbb{B}(\Delta^k, m_-^k, m_+^k, a^k)$ with aggregate model $\mathbb{U}$. Choose $a > 0$, and β^k such that $\beta^k \geq 0$ and $\sum_k \beta^k = 1$. Then $\mathbb{B}_s = \mathbb{B}(C, n_-, n_+, a) \subset \mathbb{U}$, where the parameters of $\mathbb{B}_s$ are given by

$$C = \min_k \frac{f^k}{\beta^k}, \quad n_- = \min_k \frac{m_-^k}{\beta^k}, \quad n_+ = \min_k \frac{m_+^k}{\beta^k},$$

and $f^k := \Delta^k/(1 + |1 - a/a^k|)$. $\qquad\square$

The proof of this theorem utilizes the specific assignment strategy $e^k(t) = \beta^k u(t)$. Thus, this lower bound is a sufficient condition on $u(t)$ for an aggregator to utilize the assignment $e^k(t) = \beta^k u(t)$ and achieve the desired power signal $u(t)$ in aggregate. This result is particularly useful because it specifies how the energy capacity and power limits will vary with different choices of β^k. This gives us the possibility of choosing β^k to optimize one or more of these parameters.

Lemma 1: Consider the following optimization problem

$$\max_{\beta^1,\cdots,\beta^N,n_-,n_+,C} \quad \alpha_1 n_- + \alpha_2 n_+ + \alpha_3 C$$

subject to:

$$\beta^k C \leq f^k, \qquad\qquad \forall\ k,$$
$$\beta^k n_- \leq m_-^k, \qquad\qquad \forall\ k,$$
$$\beta^k n_+ \leq m_+^k, \qquad\qquad \forall\ k,$$
$$\beta^k \geq 0, \qquad\qquad \forall\ k,$$
$$\sum_k \beta^k = 1.$$

where α_1, α_2 and α_3 are non-negative weights that negotiates the importance of n_-, n_+ and C. The optimal energy capacity C and power limits n_-, n_+ are given by

$$C = (\sum_k \gamma^k) \min_k \frac{f^k}{\gamma^k},$$

$$n_- = (\sum_k \gamma^k) \min_k \frac{m_-^k}{\gamma^k}, \quad n_+ = (\sum_k \gamma^k) \min_k \frac{m_+^k}{\gamma^k},$$

where $\gamma^k := \alpha_1 m_-^k + \alpha_2 m_+^k + \alpha_3 f^k$. $\qquad\square$

TABLE II

COMPARISON OF GENERALIZED STORAGE MODELS FOR A COLLECTION OF HETEROGENEOUS TCLs.

$\mathbb{B}_s$ (sufficient)	$\subset \mathbb{U} \subset$	$\mathbb{B}_n$ (necessary)
$\min_k \frac{f^k}{\beta^k}$	$\leq C \leq$	$\sum_k (1 + \lvert 1 - \frac{a^k}{a} \rvert) \Delta^k$
$\min_k \frac{m_-^k}{\beta^k}$	$\leq n_- \leq$	$\sum_k m_-^k$
$\min_k \frac{m_+^k}{\beta^k}$	$\leq n_+ \leq$	$\sum_k m_+^k$

Since $\mathbb{B}_n$ and $\mathbb{B}_s$ are only upper and lower bounds on $\mathbb{U}$, it is of interest to examine the gap. Table II summarizes the energy capacity and power limit gaps among $\mathbb{U}$ and $\mathbb{B}_s$, $\mathbb{B}_n$. Note that, for a population of *homogeneous* TCLs, the following corollary shows that the aggregate flexibility $\mathbb{U}$ is equivalent to a generalized battery model $\mathbb{B} = \mathbb{B}_n = \mathbb{B}_s$, i.e., $u(t) \in \mathbb{U}$ if and only if $u(t) \in \mathbb{B}$. Equivalently, it implies the gap between the battery models in Theorem 1 and Theorem 2 disappears. The proof of Corollary 1 follows immediately from Theorem 1 and Theorem 2.

Corollary 1: Consider a collection of N *homogeneous* TCLs, $\mathbb{E}^k = \mathbb{B}(\Delta, m_-, m_+, a)$ with aggregate model $\mathbb{U}$. Let $C = N\Delta$, $n_- = Nm_-$, and $n_+ = Nm_+$. Then $\mathbb{U} = \mathbb{B}(C, n_-, n_+, a)$. $\qquad\square$

V. PRIORITY-STACK-BASED CONTROL STRATEGY

In this section, we present a priority-stack-based control framework to manipulate the power consumption of a population of TCLs to provide frequency regulation service to the grid. To track a regulation signal $r(t)$, the system operator needs to determine appropriate switching actions for each TCL, so that the power deviation of TCLs, $e(t)$, follows the regulation signal $r(t)$.

We construct one ON unit stack and one OFF unit stack, as shown in Fig. 3. We assign higher priorities to the ON (OFF) units with smaller normalized temperature difference between its current temperature and the lower (upper) temperature bound. The unit with the highest priority will be turned ON (or OFF) first, and then units with lower priorities will be considered. The purpose of this priority-stack-based control strategy is to minimize the ON/OFF switching action for each unit. We index the units available for manipulation in the ON stack from *bottom to top* by $\{1, 2, \cdots, N_1\}$, and the units in the OFF available unit from *top to bottom* by $\{1, 2, \cdots, N_0\}$.
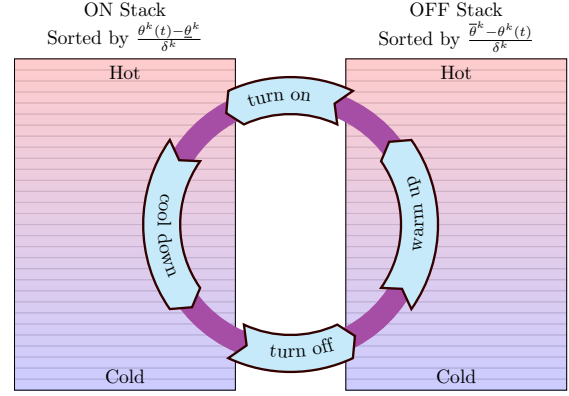

Fig. 3. The ON and OFF Priority Stacks. The lower and upper temperature bounds are given by $\underline{\theta}^k = \theta_r^k - \delta^k/2$ and $\overline{\theta}^k = \theta_r^k + \delta^k/2$ where θ_r^k is the set-point temperature of the k-th unit and δ^k is its deadband.

The priority-stack-based control algorithm is summarized in Algorithm 1. To perform such an algorithm, the following information from each TCL is needed at each sample time: (i) operating state $m^k(t)$, (ii) temperature $\theta^k(t)$, (iii) power measurement P^k, and (iv) temperature setpoint θ_r^k as well as deadband δ^k. Note that the temperature and its setpoint are readily available from the thermostat, and the operating state and deadband can be easily inferred from the past temperature measurements. At each sample time (every 4 seconds), the control algorithm first constructs the priority stacks based on the received information. It then reads the regulation signal $r(t)$ and calculates the power deviation of the population of TCLs, $e(t)$. If $e(t) < r(t)$, it searches the OFF priority stack from top to bottom such that $\sum_{i=1}^{j^*} P^i \approx r(t) - e(t)$, and then sends a switch (turn ON) signal to the units in the OFF priority stack whose index is smaller than or equal to j^*. Similarly, If $e(t) > r(t)$, it searches the ON priority stack from bottom to top such that $\sum_{i=1}^{j^*} P^i \approx e(t) - r(t)$, and then sends a switch (turn OFF) signal to the units in the ON priority stack whose index is smaller than or equal to j^*.

Algorithm 1 Priority Stack based Control Algorithm

loop
    read $m^k(t)$, $\theta^k(t)$, P^k, θ_r^k, and δ^k;
    construct priority stacks;
    obtain $r(t)$;
    compute $e(t) = P_{\text{agg}}(t) - P_0$;
    if $e(t) < r(t)$ **then**
        find $j^* = \min \{j \mid \sum_{i=1}^{j} P^i \geq r(t) - e(t)\}$;
        turn ON units indexed by $\{1, 2, \cdots, j^*\}$.
    else if $e(t) > r(t)$ **then**
        find $j^* = \min \{j \mid \sum_{i=1}^{j} P^i \geq e(t) - r(t)\}$;
        turn OFF units indexed by $\{1, 2, \cdots, j^*\}$.
    end if
end loop

VI. SIMULATION RESULTS

In this section, we apply our priority-stack-based control strategy to follow a one-hour long regulation signal (Reg

D) of PJM (Pennsylvania-New Jersey-Maryland Interconnection) [25]. The magnitude of the original signal is scaled appropriately to match the power limits and energy capacity of 1,000 TCLs. In the simulation, we use the *hybrid model* for each TCL to empirically estimate their aggregate power limits and energy capacity, and compare them with the corresponding analytic bounds of the generalized battery models developed in Theorem 1 and Theorem 2, which are developed based on the *continuous model*.

Since the gap between the (necessary) battery model $\mathbb{B}_n$ and the (sufficient) battery model $\mathbb{B}_s$ grows as the amount of heterogeneity in the TCL parameters increases, in order to obtain tighter analytic bounds on the aggregate power limits and energy capacity, one can consider clustering the population [26]. In practice, for a population of highly diverse TCLs, we can cluster the population into several groups, in which each group has similar parameter values. We then use the analytic bounds developed in Theorem 1 and Theorem 2 to estimate the aggregate flexibility of each cluster. In the simulation of this work, we consider a population of air conditioners, whose parameters are obtained by introducing a 10% of heterogeneity to the mean values of the AC parameters listed in Table I. Additionally, the ambient temperature is assumed to be $32°C$, and the initial temperatures and operating states of the population of TCLs are taken as the steady state values.

For the (necessary) battery model $\mathbb{B}_n$, its analytic lower power limit n_-, upper power limit n_+, and energy capacity C are given by

$$n_-^{(n)} = 1.9 \text{ MW}, \quad n_+^{(n)} = 3.7 \text{ MW}, \quad C^{(n)} = 0.26 \text{ MWh}.$$
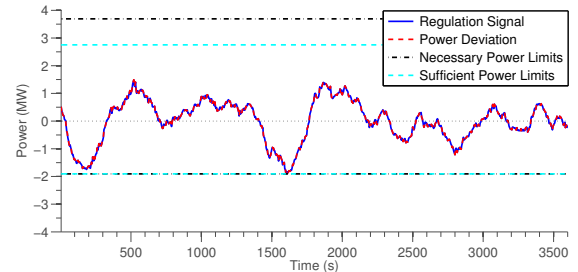
For the (sufficient) battery model $\mathbb{B}_s$, without loss of generality, we consider one of the extreme optimization cases in Lemma 1: only maximize the lower power limit n_-, i.e., let $\alpha_1 = 1, \alpha_2 = 0, \alpha_3 = 0$. In this case, the analytic lower power limit n_-, upper power limit n_+, and energy capacity C,

$$n_-^{(s)} = 1.9 \text{ MW}, \quad n_+^{(s)} = 2.8 \text{ MW}, \quad C^{(s)} = 0.19 \text{ MWh}.$$

Note that the lower power limit in the sufficient battery model $\mathbb{B}_s$ is the same as that in the necessary battery model $\mathbb{B}_n$. Fig. 4 shows that if the regulation signal's power and capacity requirements are both within the analytic bounds of the (sufficient) battery model $\mathbb{B}_s$, the population of TCLs can track it with high accuracy. The tracking error is less than 1% of the maximum magnitude of the regulation signal. Additional simulation results (not reported here) show that even with one sampling communication delay, excellent tracking is still achieved with a maximum tracking error less than 5% of the maximum magnitude of the regulation signal.

On the other hand, if either of the regulation signal's power or capacity requirements exceeds the bounds of the (necessary) battery model $\mathbb{B}_n$, the population of TCLs cannot track the regulation signal very well. Fig. 5 shows that when the regulation exceeds the power limits of the analytic bounds, the population of TCLs cannot track the regulation signal, although its capacity requirement is within the corresponding
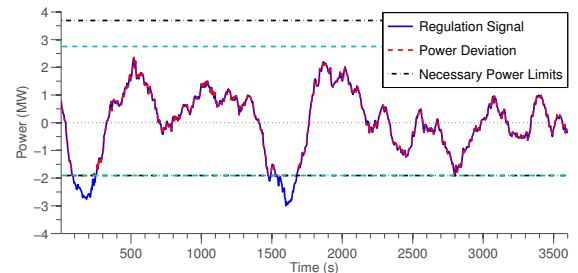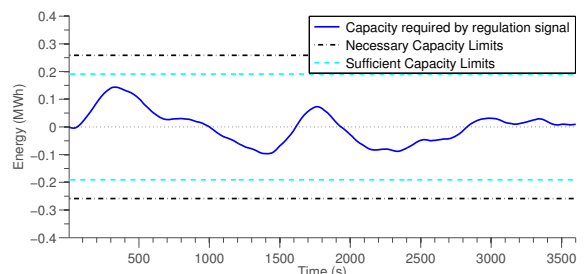

(a) Power trajectory
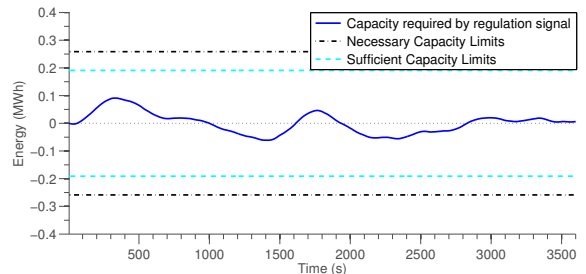
(b) Capacity trajectory

Fig. 4. Tracking of a regulation signal that is within the power limits and energy capacity of the (sufficient) battery model $\mathbb{B}_s$.
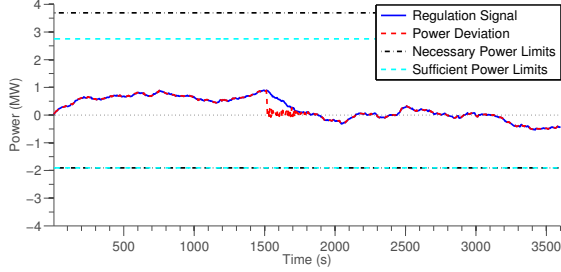

(a) Power trajectory

(b) Capacity trajectory

Fig. 5. Tracking of a regulation signal that exceeds the power limits of the (necessary) battery model $\mathbb{B}_n$.

analytic bound (Fig. 5 (b)). Additionally, Fig. 6 shows that if the capacity required by the regulation signal exceeds the capacity bound of the generalized battery model, the collection of TCLs cannot accurately track the regulation signal either, although its power requirement is within the power limits of the battery model (Fig. 6 (a)).

VII. Conclusions and Future Work

The enormous thermal storage potential of TCLs presents a tremendous opportunity for providing regulation service to the grid. In this paper, we proposed a generalized battery

(a) Power trajectory
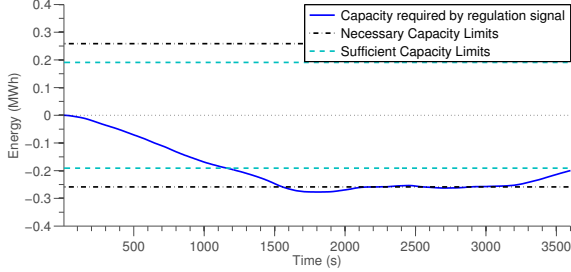
(b) Capacity trajectory

Fig. 6. Tracking of a regulation signal that exceeds the energy capacity of the (necessary) battery model $\mathbb{B}_n$.

model for aggregating flexibility of a collection of Thermostatically Controlled Loads. Based on the proposed battery model, we characterized the aggregate power limits and energy capacity for a collection of TCLs. A priority-stack-based control framework was developed to manipulate the power consumption of TCLs to track a regulation signal. We illustrated that (i) the generalized battery model provided a simple, intuitive, and powerful framework to characterize the aggregate flexibility of a population of TCLs; (ii) the analytic power and capacity bounds matched the empirically estimated bounds very well; (iii) the priority-stack-based control strategy yielded near-perfect tracking performance.

There are several future directions of interest. A theoretical justification on the approximation of a population of TCLs with the hybrid model by using the continuous model is under current investigation. A systematic characterization of the aggregate flexibility of TCLs as a function of unit participation and ambient temperature is also an ongoing work. Aggregating flexibility of other types of loads such as electric vehicles and residential pool pumps is a direction of interest.

APPENDIX

Proof of Theorem 1. The proof requires that we show that if $e^k(t) \in \mathbb{E}^k$ for all k, then $u(t) = \sum_k e^k(t) \in \mathbb{B}_n$. Assume $e^k(t) \in \mathbb{E}^k$. Let

$$\dot{\phi}^k(t) = -a^k \phi^k(t) - e^k(t), \quad \phi^k(0) = 0.$$

Taking a Laplace transform of the above equation, we obtain

$$\phi^k(s) = \frac{1}{s + a^k} e^k(s).$$

Similarly, from $\dot{x}(t) = -ax(t) - u(t)$ and $x(0) = 0$,

$$
\begin{aligned}
x(s) &= \frac{1}{s+a} u(s) = \frac{1}{s+a} \sum_k e^k(s) \\
&= \sum_k \frac{1}{s+a} e^k(s) = \sum_k \frac{s+a^k}{s+a} \frac{1}{s+a^k} e^k(s) \\
&= \sum_k \frac{s+a^k}{s+a} \phi^k(s) = \sum_k (1 + \frac{a^k - a}{s+a}) \phi^k(s).
\end{aligned}
$$

For any scalar transfer function $Y(s) = H(s)U(s)$, we have $\|y(t)\|_\infty \le \|h(t)\|_1 \|u(t)\|_\infty$, where $y(t)$, $h(t)$ and $u(t)$ are the inverse Laplace transforms of $Y(s)$, $H(s)$ and $U(s)$ respectively. Therefore,

$$\|x(t)\|_\infty \le \sum_k (1 + |1 - \frac{a^k}{a}|) \|\phi^k(t)\|_\infty.$$

Because $e^k(t) \in \mathbb{E}^k$, $\|\phi^k(t)\|_\infty \le \Delta^k$, this implies that

$$\|x(t)\|_\infty \le \sum_k (1 + |1 - \frac{a^k}{a}|) \Delta^k, \quad \forall t. \tag{9}$$

Additionally,

$$u(t) = \sum_k e^k(t), \quad -m_-^k \le e^k(t) \le m_+^k,$$

implies that

$$-\sum_k m_-^k \le u(t) \le \sum_k m_+^k. \tag{10}$$

Inequalities (9) and (10) verify that $u(t) \in \mathbb{B}_n$. ∎

Proof of Theorem 2. In this case, we must show that $u(t) \in \mathbb{B}_s = \mathbb{B}(C, n_-, n_+, a)$ implies that $e^k(t) = \beta^k u(t) \in \mathbb{E}^k = \mathbb{B}(\Delta^k, m_-^k, m_+^k, a^k)$. Now, if $u(t) \in \mathbb{B}_s$, the following must hold

$$-n_- \le u(t) \le n_+, \quad \forall t > 0$$
$$\dot{x} = -ax - u, x(0) = 0 \implies |x(t)| \le C, \quad \forall t > 0.$$

Let

$$\dot{\phi}^k(t) = -a^k \phi^k(t) - e^k(t).$$

Let $e^k(t) = \beta^k u(t)$, where $\beta^k \ge 0$, and $\sum_k \beta^k = 1$. Taking a Laplace transform of the above equation, we obtain

$$
\begin{aligned}
\phi^k(s) &= \frac{1}{s+a^k} e^k(s) = \frac{1}{s+a^k} \beta^k u(s) \\
&= \beta^k \frac{s+a}{s+a^k} \frac{u(s)}{s+a} = \beta^k (1 + \frac{a - a^k}{s+a^k}) x(s),
\end{aligned}
$$

where we have used the fact that $x(s) = \frac{1}{s+a} u(s)$. Similarly, we have

$$\|\phi^k(t)\|_\infty \le \beta^k (1 + |\frac{a - a^k}{a^k}|) \|x(t)\|_\infty$$

$$\le \beta^k (1 + |\frac{a - a^k}{a^k}|) C, \quad \forall t > 0.$$

Since C is chosen so that $\beta^k C \le f^k$, we have $|\phi(t)| \le \Delta^k$. Moreover,

$$\beta^k n_- \le m_-^k, \quad \beta^k n_+ \le m_+^k, \quad \forall k,$$

yields $-m_-^k \leq \beta^k u(t) \leq m_+^k$, and the result follows. ∎

Proof of Lemma 1. To find the maximum possible values of n_-, n_+ and C, we need to find the optimal β^k's. Since n_-, n_+ and C are all positive, we define $\psi = \frac{1}{\alpha_1 n_- + \alpha_2 n_+ + \alpha_3 C}$. Since $\beta^k n_- \leq m_-^k, \beta^k n_+ \leq m_+^k, \beta^k C \leq f^k$, we get

$$\beta^k(\alpha_1 n_- + \alpha_2 n_+ + \alpha_3 C) \leq \alpha_1 m_-^k + \alpha_2 m_+^k + \alpha_3 f^k,$$

which implies

$$\beta^k \leq (\alpha_1 m_-^k + \alpha_2 m_+^k + \alpha_3 f^k)\psi.$$

We next solve the following linear programming problem,

$$\min_{\beta^k, \psi} \quad \psi$$

subject to:

$$\beta^k \leq \gamma^k \psi, \qquad \forall\, k,$$
$$\beta^k \geq 0, \qquad \forall\, k,$$
$$\sum_k \beta^k = 1,$$

where $\gamma^k = \alpha_1 m_-^k + \alpha_2 m_+^k + \alpha_3 f^k$. Notice that if β^k's are the optimal solutions to the original optimization problem, then they are the optimal parameters to the above linear programming problem. Since $\beta^k \leq \gamma^k \psi, \ \forall k$, then

$$\sum_k \beta^k \leq \sum_k \gamma^k \psi,$$

and since $\sum_k \beta^k = 1$,

$$\psi \geq \frac{1}{\sum_k \gamma^k}, \quad \forall\, k.$$

As a result, the minimum possible value of ψ is $\frac{1}{\sum_k \gamma^k}$. The optimal β^k can now be chosen as

$$\beta^k = \frac{\gamma^k}{\sum_k \gamma^k}, \qquad \forall\, k.$$

Following straightforward algebra, the optimal solution to the original optimization problem is given by

$$C = \left(\sum_k \gamma^k\right) \min_k \frac{f^k}{\gamma^k},$$

$$n_- = \left(\sum_k \gamma^k\right) \min_k \frac{m_-^k}{\gamma^k},$$

$$n_+ = \left(\sum_k \gamma^k\right) \min_k \frac{m_+^k}{\gamma^k}.$$ ∎

REFERENCES

[1] "Mandatory renewable energy target," 2013. [Online]. Available: http://en.wikipedia.org/wiki/Mandatory_renewable_energy_target
[2] California Energy Commission, "California renewable energy overview and programs," 2013. [Online]. Available: http://www.energy.ca.gov/renewables/index.html
[3] J. Smith, M. Milligan, E. DeMeo, and B. Parsons, "Utility wind integration and operating impact state of the art," *IEEE Transactions on Power Systems*, vol. 22, no. 3, pp. 900 –908, aug. 2007.
[4] Y. Makarov, C. Loutan, J. Ma, and P. de Mello, "Operational impacts of wind generation on california power systems," *IEEE Transactions on Power Systems*, vol. 24, no. 2, pp. 1039 –1050, may 2009.
[5] S. Meyn, M. Negrete-Pincetic, G. Wang, A. Kowli, and E. Shafieepoorfard, "The value of volatile resources in electricity markets," in *CDC2010*, 2010, pp. 1029 –1036, and submitted to IEEE TAC, 2012.
[6] U. Helman, "Resource and transmission planning to achieve a 33% RPS in California–ISO modeling tools and planning framework," in *FERC Technical Conference on Planning Models and Software*, 2010.
[7] Market and Infrastructure Policy, "2013 flexible capacity procurement requirement," Tech. Rep., March 2012. [Online]. Available: http://www.CAISO.com/
[8] "Buildings energy data book." [Online]. Available: http://buildingsdatabook.eren.doe.gov/default.aspx
[9] "U.S. Energy Information Administration, annual energy review," 2010. [Online]. Available: http://www.eia.gov/totalenergy/data/annual/#consumption
[10] S. Ihara and F. C. Schweppe, "Physically based modeling of cold load pickup," *Power Apparatus and Systems, IEEE Transactions on*, no. 9, pp. 4142–4150, 1981.
[11] R. Malhame and C.-Y. Chong, "Electric load model synthesis by diffusion approximation of a high-order hybrid-state stochastic system," *Automatic Control, IEEE Transactions on*, vol. 30, no. 9, pp. 854–860, 1985.
[12] D. S. Callaway, "Tapping the energy storage potential in electric loads to deliver load following and regulation, with application to wind energy," *Energy Conversion and Management*, vol. 50, no. 5, pp. 1389–1400, 2009.
[13] S. Kundu, N. Sinitsyn, S. Backhaus, and I. Hiskens, "Modeling and control of thermostatically controlled loads," in *the 17-th Power Systems Computation Conference*, 2011.
[14] S. Koch, J. Mathieu, and D. Callaway, "Modeling and control of aggregated heterogeneous thermostatically controlled loads for ancillary services," in *Proc. PSCC*, 2011, pp. 1–7.
[15] S. Bashash and H. K. Fathy, "Modeling and control insights into demand-side energy management through setpoint control of thermostatic loads," in *American Control Conference (ACC), 2011.* IEEE, 2011, pp. 4546–4553.
[16] W. Zhang, K. Kalsi, J. Fuller, M. Elizondo, and D. Chassin, "Aggregate model for heterogeneous thermostatically controlled loads with demand response," in *Power and Energy Society General Meeting, 2012 IEEE.* IEEE, 2012, pp. 1–8.
[17] J. L. Mathieu, S. Koch, and D. S. Callaway, "State estimation and control of electric loads to manage real-time energy imbalance," *IEEE Transactions on Power Systems*, vol. 28, no. 1, pp. 430 –440, Feburary 2013.
[18] J. L. Mathieu, M. Kamgarpour, J. Lygeros, and D. S. Callaway, "Energy arbitrage with thermostatically controlled loads," in *European Control Conference (ECC)*, 2013.
[19] S. Meyn, P. Barooah, A. Busic, and J. Ehren, "Ancillary service to the grid from deferrable loads: the case for intelligent pool pumps in florida," in *IEEE conference on Decision and Control (CDC), submitted*, 2013.
[20] Pacific Gas and Electric Company, "Smart AC program." [Online]. Available: http://www.pge.com/en/myhome/saveenergymoney/energysavingprograms/smartac/index.page
[21] B. Kirby, "Ancillary services: Technical and commercial insights," Tech. Rep., July 2007.
[22] "Storage participation in ERCOT, prepared by the texas energy storage alliance," January 2010. [Online]. Available: http://www.ercot.com/
[23] H. Hao, B. M. Sanandaji, K. Poolla, and T. L. Vincent, "Frequency regulation from flexible loads: Potential, economics, and implementation," *submitted to American Control Conference*, September 2013. [Online]. Available: http://plaza.ufl.edu/hehao/publication.html
[24] J. Mathieu, M. Dyson, and D. Callaway, "Using residential electric loads for fast demand response: The potential resource and revenues, the costs, and policy recommendations," in *2012 ACEEE Summer Study on Energy Efficiency in Buildings*, 2012.
[25] "PJM regulation data." [Online]. Available: http://www.pjm.com/markets-and-operations/ancillary-services/mkt-based-regulation/fast-response-regulation-signal.aspx
[26] B. M. Sanandaji, H. Hao, K. Poolla, and T. L. Vincent, "Improved battery models of an aggregation of thermostatically controlled loads for frequency regulation," *submitted to American Control Conference*, September 2013. [Online]. Available: http://plaza.ufl.edu/hehao/publication.html